

View Invariants for Three-Dimensional Points with Constrained Observer Motion

Paul D. McKee*

Rensselaer Polytechnic Institute, Troy, New York 12180

Harm Derksen†

Northeastern University, Boston, Massachusetts 02115

and

John A. Christian‡

Georgia Institute of Technology, Atlanta, Georgia 30332

https://doi.org/10.2514/1.G006793

Images from cameras are a common source of navigation information for a variety of vehicles. Such navigation often requires the matching of observed objects (e.g., landmarks, beacons, stars) in an image to a catalog (or map) of known objects. In many cases, this matching problem is made easier through the use of invariants. However, if the objects are modeled as three-dimensional points in general position, it has long been known that there are no invariants for a camera that is also in general position. This work discusses how invariants are introduced when the camera's motion is constrained to a line, and proves that this is the only camera path along which invariants are possible. Algorithms are presented for computing both the invariants and the location for a camera undergoing rectilinear motion. The applicability of these ideas is discussed within the context of trains, aircraft, and spacecraft.

I. Introduction

I DENTIFYING objects in a digital image is a common task for vision-based perception systems. In many cases, invariant theory [1-5] provides a powerful framework for accomplishing this task. The idea is to find and catalog properties of an object (or group of objects) that remain unchanged when the object is viewed by a camera from different viewpoints. Of particular interest here are view invariants, which describe those invariants that may be constructed exclusively from information contained within an image. Thus, regardless of how the object is oriented relative to the camera when the image is taken, one may always compute the same numerical values for the view invariants. If these view invariants are unique for each object, they provide an easy means of image-based object identification. Such an interpretation and use of invariants is wellestablished [6-9], and has seen widespread use in both terrestrial and space applications. For example, invariants have been used in spacecraft navigation to identify star patterns [10,11] or planetary landmarks (e.g., craters [12]) in digital images taken by space cameras. They can also be used to recognize patterns of retroreflectors seen in Flash LIDAR images [13], such as during the rendezvous with a cooperative spacecraft [14].

Despite the utility of invariants for object recognition and its great success in solving some problems (e.g., star pattern recognition), invariants do not exist for all types of objects or all classes of motion. Perhaps the most well-known example of a scenario lacking invariants is a cloud of arbitrary three-dimensional (3-D) points as imaged from a camera of arbitrary position. Indeed, this lack of nontrivial, general-case view invariants may be proven in a number of different ways [11,12,15,16]. The prevalence of scenarios with cameras

viewing objects that can be modeled as 3-D points makes this result disheartening.

Fortunately, invariants may be introduced by placing constraints on either the 3-D point configuration or the observer's motion. For example, if an uncalibrated camera in general position observes a d-tuple of points constrained to lie on a plane, then there are known to be 2d-8 invariants [17]. Alternatively, if the d-tuple of points are in general position but the camera has a fixed location (but unknown orientation), there are 2d-3 invariants for a calibrated camera and 2d-8 invariants for an uncalibrated camera [10]. To complement these known results, this work explores the existence of invariants for a d-tuple of 3-D points in general position as seen by an observer constrained to move along a known path. Such a scenario is important since design or selection of the 3-D points is often outside of the user's control

This work presents three key results. The first key result is that there exist no view invariants for a moving camera observing 3-D points unless all the camera positions are colinear. Thus, rectilinear motion is the only camera motion that permits view invariants for observations of 3-D points in general position. The second key result is that there are *d* independent view invariants for a *d*-tuple of 3-D points seen by a calibrated camera of known attitude that is constrained to move along a known line. These invariants may be computed from a catalog of 3-D point locations or from the apparent location of points in an image. The third key result is that the new invariants discussed here have a wide variety of practical applications. Indeed, although this work was first motivated by the problem of star identification in interstellar space [11], the results shown here have several other potential aerospace and transportation applications. Some example applications are discussed.

II. Background

The proper development of invariants for a particular object recognition problem contains at least two primary steps. The first step is the enumeration of the number of fundamental invariants. This ensures that the problem is solvable (i.e., that invariants actually exist) and lets the analyst know how many independent invariants must be found. The second step is to find ways of computing the desired invariants from the observations. Of the two steps, it is the first step that requires the most careful review of invariant theory. This background section provides such a review. For more details on this topic see Ref. [9].

Received 1 March 2022; revision received 12 August 2022; accepted for publication 29 August 2022; published online 17 October 2022. Copyright © 2022 by Paul D. McKee, Harm Derksen, and John A. Christian. Published by the American Institute of Aeronautics and Astronautics, Inc., with permission. All requests for copying and permission to reprint should be submitted to CCC at www.copyright.com; employ the eISSN 1533-3884 to initiate your request. See also AIAA Rights and Permissions www.aiaa.org/randp.

^{*}Ph.D. Candidate, Mechanical, Aerospace, and Nuclear Engineering Department.

[†]Professor, Department of Mathematics.

[‡]Associate Professor, Guggenheim School of Aerospace Engineering. Associate Fellow AIAA.

A. Fundamental Invariants, Rational Invariants, and Indexing

An invariant is a function on an algebraic variety whose output does not change when some group acts on the variety. These ideas have their root in early work by Hilbert [18,19] and have been studied extensively since then [3,5]. To explore these concepts more fully, suppose that $\mathcal V$ is an irreducible algebraic variety. Then, let $\mathbb C(\mathcal V)$ denote the set of all rational functions on $\mathcal V$ over the complex numbers $\mathbb C$. This set has the algebraic structure of a field. Further, denote $\mathbb C(\mathcal V)^{\mathcal G}$ as the set of all functions on the variety $\mathcal V$ that are invariant under the action of group $\mathcal G$. It follows that $\mathbb C(\mathcal V)^{\mathcal G}$ is a subfield of $\mathbb C(\mathcal V)$.

If $f_1, f_2, \dots, f_n \in \mathbb{C}(\mathcal{V})^{\mathcal{G}}$, then f_1, f_2, \dots, f_n are called fundamental invariants if every other invariant rational function can be expressed uniquely as an algebraic function in f_1, f_2, \dots, f_n . This also means that there should not be any algebraic relations between f_1, f_2, \ldots, f_n . In the language of field theory, f_1, f_2, \dots, f_n are fundamental invariants exactly when they form a transcendence basis of the field $\mathbb{C}(\mathcal{V})^{\mathcal{G}}$ over \mathbb{C} . Suppose that f_1, f_2, \ldots, f_n are fundamental invariants. The set of all functions that are rational expressions form a field $\mathbb{C}(f_1, f_2, \ldots, f_n)$ and $\mathbb{C}(\mathcal{V})^{\mathcal{G}}$ is an algebraic field extension of $\mathbb{C}(f_1,\ldots,f_n)$. This means that every invariant $g \in \mathbb{C}(\mathcal{V})^{\mathcal{G}}$ satisfies an equation of the form $g^d + a_{d-1}(f_1, \dots, f_n)g^{d-1} + \dots + a_0(f_1, \dots, f_n),$ where a_0 , a_1, \ldots, a_{d-1} are rational functions. In particular, if the function values of f_1, f_2, \ldots, f_n are fixed, then there are at most finitely many possible values of g. It is possible though that the field $\mathbb{C}(f_1,\ldots,f_n)$ is a proper subfield of $\mathbb{C}(\mathcal{V})^{\mathcal{G}}$. That is, there may be invariants that are not a rational expression in f_1, \ldots, f_n , even though they are an algebraic function in f_1, \ldots, f_n .

If there are n fundamental invariants, that means there are n algebraically independent functions on the algebraic variety \mathcal{V} that are invariant under the action of group \mathcal{G} [1–3]. While the analyst is free to choose which functions are the fundamental invariants and which are secondary functions, only n are algebraically independent. If one chooses to compute m > n invariants, they will find that at least m-n of these invariants contain redundant information. If one chooses to compute p < n invariants, they are leaving out n-p pieces of potentially useful information. The n fundamental invariants may be used to populate an n-dimensional index space for the purposes of object recognition [7].

B. Finding the Number of Fundamental Invariants

In some cases there may be no fundamental invariants or no finite set of fundamental invariants, or the number of fundamental invariants may be much larger than the dimension of the space [20]. Thus, it is a nontrivial result to find that there is a small (i.e., practical) number of fundamental invariants that can be used in an object recognition problem.

One can view $\mathbb{C}(\mathcal{V})^{\mathcal{G}}$ as a field extension over \mathbb{C} . The transcendence degree of a field extension can be thought of as an approximation of its size [21], mirroring the idea of dimension in linear algebra. Consider a field L having a subfield K. The transcendence degree of L over K, denoted as $\operatorname{trdeg}(L/K)$, is the largest cardinality of any subset of L that is algebraically independent over K.

Proceed by first reviewing a few facts about the transcendence degree. If a field extension is purely algebraic, meaning that it has no transcendental elements, it has a transcendence degree of zero. If K is a field and x_1, \ldots, x_n are n indeterminates, then $K(x_1, \ldots, x_n)$ is the field of rational functions in n variables x_1, \ldots, x_n over K. The transcendence degree of the field extension $K(x_1, \ldots, x_n)/K$ is

$$\operatorname{trdeg}(K(x_1, \dots, x_n)/K) = n \tag{1}$$

If V is an algebraic variety, then

$$\operatorname{trdeg}(\mathbb{C}(\mathcal{V})/\mathbb{C}) = \dim(\mathcal{V}) \tag{2}$$

Further, if L is a field extension over K and M is a field extension over L, then

$$trdeg(M/K) = trdeg(M/L) + trdeg(L/K)$$
 (3)

The maximum number of fundamental invariants is related to the idea of the transcendence degree of a field extension. Specifically, $\operatorname{trdeg}(\mathbb{C}(\mathcal{V})^{\mathcal{G}}/\mathbb{C})$ is the maximum number of rational invariants that are algebraically independent. If L is an extension field of K and the functions $f_1, \ldots, f_n \in L$ are algebraically independent over K, then $\operatorname{trdeg}(L/K)$ is the maximum possible value of n.

III. Existence of View Invariants

The first task for invariant-based object recognition is to establish the existence of invariants. This depends on the specifics of the scenario under consideration. Therefore, this analysis begins by a description of the problem geometry and is followed by an enumeration of the number of fundamental invariants. The number of fundamental invariants is found to be finite and nonzero for a calibrated camera undergoing rectilinear motion.

A. Problem Geometry: Rectilinear Motion of a Calibrated Camera

Consider the case of an observer constrained to motion along a line. To describe this observer's position (and without loss of generality), define an inertial reference frame whose z axis coincides with the observer's line of motion. It follows that the observer's position may be written as $r = [0, 0, r]^T$.

Now, suppose that this observer is equipped with a calibrated camera capable of producing bearing measurements to a d-tuple of points in general position. Let the position of the ith point be denoted as $\mathbf{p}_i = [x_i, y_i, z_i]^T \in \mathbb{R}^3$. Thus, bearing measurement describes the line $\mathcal{C}_i \in \mathbb{P}^2$ that connects the observer's location at some instant in time (\mathbf{r}) with the observed point (\mathbf{p}_i) . A point along this line may be computed as

$$\mathcal{C}_i \propto \mathbf{p}_i - \mathbf{r} = \begin{bmatrix} x_i \\ y_i \\ z_i - r \end{bmatrix} \tag{4}$$

The proportional relationship is a compact way of capturing the pinhole camera geometry. This approach prevents unnecessary normalizations and often simplifies the mathematics (see Ref. [22] for details). This problem geometry is illustrated in Fig. 1.

If the observer's camera is calibrated and has a known attitude, then there is a one-to-one mapping between the direction \mathcal{E}_i and the apparent location of that point in a digital image. To make this relationship explicit, first recognize that the vector \mathcal{E}_i is of arbitrary scale and is expressed in the inertial frame. Thus, the image plane coordinate $[x_i, y_i]$ where the direction to p_i pierces the camera frame's z=1 plane is given by

$$\begin{bmatrix} x_i \\ y_i \\ 1 \end{bmatrix} = \bar{x}_i \propto T \mathcal{C}_i \tag{5}$$

where $T \in SO(3)$ is an attitude transformation matrix that rotates a vector expressed in the inertial frame into the camera frame.

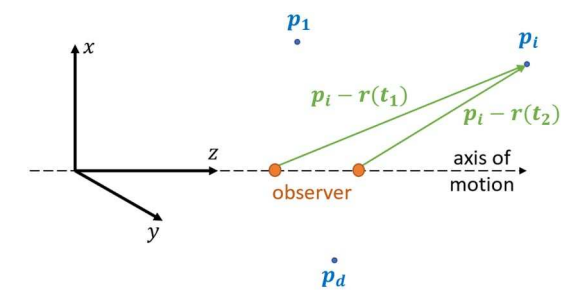


Fig. 1 An observer moving along the z-axis takes bearing measurements to the 3-D point p_i , which is one of multiple arbitrary points $p_1, \ldots, p_i, \ldots, p_d$ in 3-D space.

The matrix T is presumed known in this problem. Next, recall that the homogeneous image plane coordinate \bar{x}_i may be related to the pixel coordinate $[u_i, v_i]$ in a digital image by

$$\begin{bmatrix} u_i \\ v_i \\ 1 \end{bmatrix} = \bar{\boldsymbol{u}}_i = \boldsymbol{K}\bar{\boldsymbol{x}}_i \tag{6}$$

The 3×3 matrix **K** is the camera calibration matrix and describes an affine transformation of the form

$$\mathbf{K} = \begin{bmatrix} d_x & \alpha & u_p \\ 0 & d_y & v_p \\ 0 & 0 & 1 \end{bmatrix} \tag{7}$$

where d_x is the ratio of focal length to pixel pitch in the x-direction (d_y) is the same thing in the y-direction), α describes the detector skewness, and $[u_p, v_p]$ is pixel coordinate of the principal point [22,23]. Therefore, substituting Eq. (6) into Eq. (5), the pixel coordinates of the point $[u_i, v_i]$ in an image may be related to \mathcal{C}_i by the homography $\mathbf{H} \propto \mathbf{KT}$,

$$\begin{bmatrix} u_i \\ v_i \\ 1 \end{bmatrix} = \bar{\boldsymbol{u}}_i \propto \boldsymbol{H}\boldsymbol{\ell}_i \propto \boldsymbol{K}\boldsymbol{T}\boldsymbol{\ell}_i \tag{8}$$

The matrix K is known if the camera is calibrated, and its inverse may be computed analytically (see [22]). It follows that the inverse homography $H^{-1} = T^T K^{-1}$ is known and may also be computed analytically. Thus, given the apparent pixel location $[u_i, v_i]$, one may compute the inertial direction \mathscr{E}_i directly as

$$\mathcal{E}_i \propto H^{-1} \bar{u}_i = T^T K^{-1} \begin{bmatrix} u_i \\ v_i \\ 1 \end{bmatrix}$$
 (9)

where the scaling of \mathcal{C}_i is unimportant. Common conventions are to make \mathcal{C}_i a unit vector or to set the *z*-component to unity, but this choice is unimportant here. The solutions and results that follow will work for any choice of normalization.

B. Finding the Number of Fundamental Invariants

Let *L* be the field generated by the 3-D location of each point and the 3-D position of the observer:

$$L = \mathbb{C}(x_1, y_1, z_1, \dots, x_d, y_d, z_d, r)$$
 (10)

Any functions that are invariant to changes in observer position must be a subset of L. Let K_1 and K_2 be subfields of L that contain \mathbb{C} , the complex numbers.

The invariants of interest are those that can be generated from observations in an image (i.e., the view invariants). Thus, define the subfield K_1 as the field generated by only the point observations in an image

$$K_1 = \mathbb{C}(u_1, v_1, \dots, u_d, v_d)$$
 (11)

Next, define the subfield K_2 as the field generated by the 3-D position components of each point:

$$K_2 = \mathbb{C}(x_1, y_1, z_1, \dots, x_d, y_d, z_d)$$
 (12)

The intersection field $K = K_1 \cap K_2$ is the field generated by the catalog position of each point and the measurement of each point but not the observer position. Any fundamental invariants that may be used to identify the d-tuple of points (functions whose output is invariant to changes in observer position) must lie in K. To proceed, one must know the number of functions that generate K. Application of Eq. (1) shows that

$$\operatorname{trdeg}(K/\mathbb{C}) = \operatorname{trdeg}(\mathbb{C}(f_1, \dots, f_n)) = n \tag{13}$$

where f_1, \ldots, f_n are the fundamental invariant functions and n is the number of fundamental invariants for this problem. Ultimately, n can be determined by finding $\operatorname{trdeg}(K/\mathbb{C})$. Recall from Eq. (3) that transcendence degrees of field extensions add, such that

$$\operatorname{trdeg}(L/\mathbb{C}) = \operatorname{trdeg}(L/K) + \operatorname{trdeg}(K/\mathbb{C}) \tag{14}$$

Thus, the number of fundamental invariants may be computed as

$$n = \operatorname{trdeg}(K/\mathbb{C}) = \operatorname{trdeg}(L/\mathbb{C}) - \operatorname{trdeg}(L/K)$$
 (15)

To find the number of fundamental invariants, n, one must compute both $\operatorname{trdeg}(L/\mathbb{C})$ and $\operatorname{trdeg}(L/K)$. The former is easy and the latter requires a little more development. Specifically, it is straightforward to show that $\operatorname{trdeg}(L/\mathbb{C}) = 3d + 1$ from the definition of L and Eq. (1). Attention is now turned to the further development of $\operatorname{trdeg}(L/K)$.

1. Analysis of trdeg(L/K)

The field L is an extension field of K, and K is a subfield of L. A derivation on K is a function $D:L \to L$ that satisfies Leibniz's rule D(ab) = aD(b) + bD(a). The subfield K lies in the kernel of L if and only if D(K) = 0. In this case, D is called a K-derivation. The space of all K-derivations, denoted as $\mathrm{Der}_K(L)$, is an L-vector space with dimension given by

$$\dim(\operatorname{Der}_{K}(L)) = \operatorname{trdeg}(L/K) \tag{16}$$

as follows from Theorem 23.12 in Ref. [24].

Thus, define the derivative function

$$D_i := x_i \left(\frac{d}{dx_i}\right) + y_i \left(\frac{d}{dy_i}\right) + (z_i - r) \left(\frac{d}{dz_i}\right) \tag{17}$$

for $i = 1, \ldots, d$. Recall that K_1 is generated by u_i and v_i . The field K_1 lies in the kernel of D_i for all i. Recall that K_2 is generated by x_i, y_i, z_i and not by r. As such, K_2 lies in the kernel of the derivation d/dr. Because K lies in the intersection of K_1 and K_2 , it lies in the kernels of D_1, \ldots, D_d and d/dr.

The Lie bracket of two K-derivations is another K-derivation. Therefore, it can be said that K does not just lie in the kernel of D_1, \ldots, D_d and d/dr, but in the kernel of all K-derivations in the Lie Algebra generated by these. The Lie algebra generated by $D_1, D_2, \ldots, D_d, d/dr$ contains $[D_i, d/dr] = d/dz_i$ and $D_i - (z_i - r)d/dz_i = x_id/dx_i + y_id/dy_i$ for all i. So this Lie Algebra contains the (2d+1) derivations

$$\left(\frac{d}{dz_1}\right), \dots, \left(\frac{d}{dz_d}\right), \left(\frac{d}{dr}\right), x_1\left(\frac{d}{dx_1}\right) + y_1\left(\frac{d}{dy_1}\right), \dots, x_d\left(\frac{d}{dx_d}\right) + y_d\left(\frac{d}{dy_d}\right)$$
(18)

that are linearly independent over L. Thus, it can be said that $\dim(\operatorname{Der}_K(L)) \geq 2d+1$. Moreover, combining with Eq. (16), one finds that

$$\operatorname{trdeg}(L/K) = \dim(\operatorname{Der}_K(L)) \ge 2d + 1 \tag{19}$$

2. Number of Fundamental Invariants

It is now possible to compute the number of fundamental invariants. To accomplish this, first recall that $\operatorname{trdeg}(L/\mathbb{C})=3d+1$. Substitute this result, along with the results of Eq. (19), into Eq. (15) to find

$$n = \operatorname{trdeg}(K/\mathbb{C}) = \operatorname{trdeg}(L/\mathbb{C}) - \operatorname{trdeg}(L/K)$$

$$\leq (3d+1) - (2d+1) = d$$
(20)

Hence, one finds the number of fundamental invariants to be $n \le d$. Consequently, for the problem of bearing measurements to a d-tuple of 3-D points in general position as seen by an observer constrained to a line, there are at most d fundamental invariant functions that may be useful for point identification.

C. Nonexistence of Invariants for Nonlinear Paths

Section III considered the case of a calibrated camera of known attitude moving along a line. An interesting question is whether it is also possible to find invariants when the observer is moving along some other type of path (e.g., along a conic orbit). It was found that such invariants do not exist. This will now be shown.

Consider three possible positions of the camera: q, q', and q''. A 3-D point p_i corresponds to pixel locations $[u_i, v_i]$, $[u_i', v_i']$, and $[u_i'', v_i'']$ in the images from the cameras at positions q, q', and q'', respectively. An invariant is a function that can be computed from each of the camera images independently. Thus, an invariant is a function $g(x_1, y_1, z_1, \ldots, x_d, y_d, z_d)$ such that there are functions f, f', and f'' such that

$$g(x_1, y_1, z_1, \dots, x_d, y_d, z_d) = f(u_1, v_1, \dots, u_d, v_d)$$

= $f'(u'_1, v'_1, \dots, u'_d, v'_d)$
= $f''(u''_1, v''_1, \dots, u''_d, v''_d)$

It is now possible to show that there exists a nontrivial invariant if and only if q, q', and q'' are colinear. Since these three camera positions are arbitrary, the constraint that they are colinear means that the entire trajectory must be constrained to a line. Let $L = \mathbb{C}(x_1, y_1, z_1, \ldots, x_d, y_d, z_d)$ and consider the subfields

$$K = \mathbb{C}(u_1, v_1, \dots, u_d, v_d), K' = \mathbb{C}(u'_1, v'_1, \dots, u'_d, v'_d),$$
 and $K'' = \mathbb{C}(u''_1, v''_1, \dots, u''_d, v''_d)$

There exists a nontrivial rational invariant if and only if $K \cap K' \cap K'' \neq \mathbb{C}$. Let $\mathbf{q} = [\alpha, \beta, \gamma]^T$, $\mathbf{q}' = [\alpha', \beta', \gamma']^T$, and $\mathbf{q}'' = [\alpha'', \beta'', \gamma'']^T$. Thus, the derivations

$$D_i := (x_i - \alpha) \left(\frac{d}{dx_i}\right) + (y_i - \beta) \left(\frac{d}{dy_i}\right) + (z_i - \gamma) \left(\frac{d}{dz_i}\right)$$
 (21)

for i = 1, 2, ..., d are derivations on L over the field K. Similarly, one may define the derivations $D'_i \in \text{Der}_{K'}(L)$ and $D''_i \in \text{Der}_{K''}(L)$.

Suppose that q, q', and q'' are not colinear. If $r := [x_i, y_i, z_i]^T$ is a point that is not in the plane through q, q', q'', then the vectors $r - q = [x_i - \alpha, y_i - \beta, z_i - \gamma]^T, r - q'$, and r - q'' are linearly independent. It follows that D_i, D_i', D_i'' are linearly independent over L. In particular $d/dx_i, d/dy_i, d/dz_i$ lie in the L-linear span of D_i, D_i', D_i'' . The field $K \cap K' \cap K''$ lies in the kernel of all the derivations $d/dx_i, d/dy_i, d/dz_i$ on L with $1 \le i \le d$ and therefore must be equal to $\mathbb C$. Hence, there are no invariants in this case.

Conversely, if q, q', q'' are colinear, then it is possible to view q, q', and q'' as different locations within a linear motion of the observer, and it has already been shown that there are nontrivial invariants in this case (see Sec. III).

IV. Using Invariants for Point Identification

The existence of view invariants makes efficient object recognition possible. The idea is to first precompute the invariants of *known* objects and store these results in an index. Then, when supplied with an image, the invariants of *observed* objects may be computed in real-time. These observation invariants can be used to perform a range query on the index, returning all possible index entries (corresponding to catalog objects) having invariants within a specified tolerance of the query point. This concept is well-established in classical computer vision [17], and such an abstraction was subsequently explored for a variety of object recognition problems in space exploration [10,12].

Adopting this approach, a scheme for point identification requires a means for 1) computing invariants from the point catalog, 2) computing invariants from bearing measurements, and 3) performing the range query. Each of these topics is now discussed in more detail.

A. Computing Invariants from 3-D Point Catalog

By construction, the observer's motion is constrained to lie along the z-axis. Thus, defining the z-axis with the unit vector $k = [0, 0, 1]^T$, the observer's position may be written as r = rk. If the *i*th observed point does not lie along the z-axis, then the vector p_i and r span a plane in \mathbb{R}^3 . This plane has a normal vector n_i (see Fig. 2), which may be computed as

$$n_i \propto r \times p_i \propto k \times p_i$$
 (22)

Recognizing that the normal vector \mathbf{n}_i is perpendicular to the z-axis by construction, it is observed that the plane orientation has only one degree of freedom. This single degree of freedom may be described in many ways, with one of the simplest being the angle between the x-axis and \mathbf{n}_i (called the clocking angle). This angle may be computed as

$$\tan(\theta_i) = \frac{\boldsymbol{n}_i^T \boldsymbol{j}}{\boldsymbol{n}_i^T \boldsymbol{i}} \tag{23}$$

where $i = [1, 0, 0]^T$, $j = [0, 1, 0]^T$, and the scaling of n_i doesn't matter. Hence, substituting from Eq. (22) and making use of the triple product, one finds that

$$\tan(\theta_i) = \frac{(\mathbf{r} \times \mathbf{p}_i)^T \mathbf{j}}{(\mathbf{r} \times \mathbf{p}_i)^T \mathbf{i}} = \frac{(\mathbf{k} \times \mathbf{p}_i)^T \mathbf{j}}{(\mathbf{k} \times \mathbf{p}_i)^T \mathbf{i}} = -\frac{\mathbf{p}_i^T \mathbf{i}}{\mathbf{p}_i^T \mathbf{j}} = -\frac{x_i}{y_i}$$
(24)

Recall here the assumption that each point p_i is in general position. For any point p_i lying along the line of vehicle motion (i.e., $p_i \propto r \propto k$), then $x_i = y_i = 0$ and the clocking angle θ_i is undefined. Thus, while one cannot form the invariant from Eq. (24) for a point along (or nearly along) the direction of observer motion, the constant bearing of $x_i = y_i = 0$ is itself an invariant for this degenerate case. Thus, assuming a point p_i in general position, Eq. (24) may be solved for θ_i using a four-quadrant inverse tangent function, such as atan2. The angle θ_i does not depend on the observer location along the line r = rk, but is only a function of the location of point p_i . Hence, the angle θ_i is a view invariant under the assumed motion. The result of Eq. (24) may be used to precompute the invariant corresponding to each catalog point using only the catalog data.

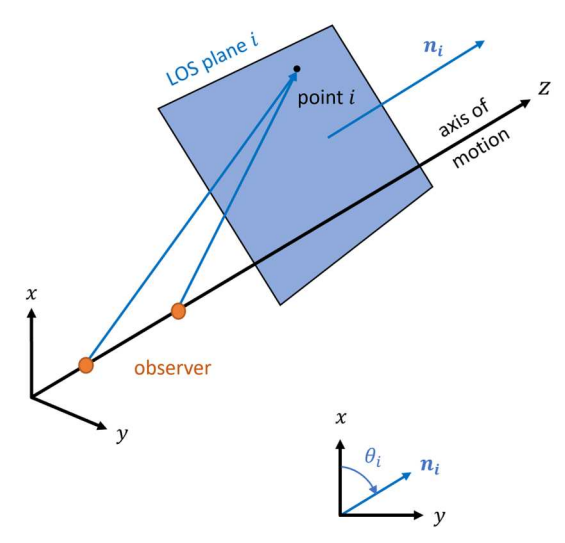


Fig. 2 All possible unit vectors from the observer to point *i* lie in a plane that is invariant to observer motion along the *z*-axis.

B. Computing Invariants from Bearing Observations

The result of Eq. (24) describes how to compute the unique invariant for each 3-D point using only the location of that point. For efficient recognition to be possible, it is necessary to compute the invariant from Eq. (24) using only the corresponding bearing observation. Thus, returning to Eq. (22), note that the normal may be rewritten in terms of the measured bearing vector \mathcal{E}_i :

$$\mathbf{n}_i \propto \mathbf{k} \times \mathbf{p}_i = \mathbf{k} \times (\mathbf{p}_i - \mathbf{r}) \propto \mathbf{k} \times \mathbf{\ell}_i$$
 (25)

which makes use of the relationship from Eq. (4). Substituting this result into Eq. (24),

$$\tan(\theta_i) = \frac{\mathbf{n}_i^T \mathbf{j}}{\mathbf{n}_i^T \mathbf{i}} = -\frac{\mathcal{C}_i^T \mathbf{i}}{\mathcal{C}_i^T \mathbf{j}}$$
(26)

where $i = [1, 0, 0]^T$, $j = [0, 1, 0]^T$, and the scaling of \mathcal{E}_i doesn't matter. The bearing measurements \mathcal{E}_i could come from any sensor observing the direction from the vehicle to the 3-D point p_i . However, assuming that the sensor is a camera, one can write \mathcal{E}_i directly in terms of the observed image coordinates $\bar{u}_i^T = [u_i, v_i, 1]$ and the known homography $H \propto KT$ using Eq. (9). Making this substitution,

$$\tan(\theta_i) = -\frac{\boldsymbol{\ell}_i^T \boldsymbol{i}}{\boldsymbol{\ell}_i^T \boldsymbol{j}} = -\frac{\bar{\boldsymbol{u}}_i^T \boldsymbol{H}^{-T} \boldsymbol{i}}{\bar{\boldsymbol{u}}_i^T \boldsymbol{H}^{-T} \boldsymbol{j}}$$
(27)

This allows for computation of the invariant θ_i using atan2 (or similar) with only the bearing measurement. The bearing measurement may be written either in terms of the direction \mathcal{E}_i (which is expressed in the inertial frame and has arbitrary scale) or explicitly in terms of camera pixel coordinates \bar{u}_i .

C. Recognition Using Invariants

It is known from Eq. (20) that there are $n \le d$ fundamental invariants for bearing measurements to a d-tuple of points by an observer whose location is constrained to a line. Observing, therefore, that Eqs. (24) and (27) describe d independent invariants, it follows that there are exactly n = d fundamental invariants. Moreover, since Eq. (24) is only a function of the ith point p_i [and, likewise, Eq. (27) is only a function of the ith bearing measurement \mathcal{C}_i], there is one invariant associated with each point and this invariant is independent of all other points.

Given a d-tuple of points, each point has a 1-D invariant that may be used to recognize this point. If the invariant associated with a single bearing measurement is computed using Eq. (27), then this numerical value may be used to query an index of all the invariants belonging to catalog points as computed using Eq. (24). The objective is to return all catalog points having an invariant within a specified tolerance of the query point—which is equivalent to returning all catalog points having an invariant between a minimum and maximum value. This is a classical range query problem [25,26]. Further, since this is a 1-D range query, there are a number of data structures that are especially efficient for 1-D range queries, such as the k-vector [27–29].

The scalar invariants $\{\theta_i\}_{i=1}^d$ are constrained to real numbers between zero and 2π . If a very large number of 3-D points are in the catalog, there may not be much angular separation between the 1-D invariants that form the index entries. Thus, if the measurement error used to define the bounds of the range query is not small compared to the index spacing, it is possible that multiple catalog entries will be returned (as illustrated in Fig. 3). In this case, additional information would be required to eliminate ambiguity in the point match. It is usually best to design the system to avoid this situation whenever possible.

V. Observer Position Estimation

The *d* bearing measurements $\{\mathcal{E}_i\}_{i=1}^d$ to the *d*-tuple of 3-D points $\{p_i\}_{i=1}^d$ may be used to estimate the observer's location via triangulation. Methods in triangulation are well established [30] and have

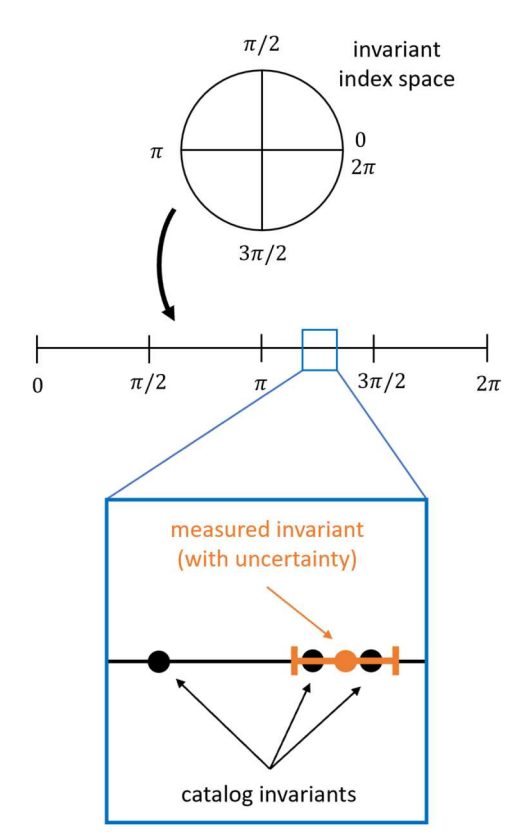


Fig. 3 It is possible for a range query to return multiple matches if the uncertainty in the measured invariant is larger than the spacing between catalog invariants.

been widely explored within the context of space exploration [31,32]. The most common, simple, and scalable triangulation method is the so-called direct linear transform (DLT)—and this is the method used here. The DLT solution takes on an especially elegant form in this problem since the observer motion is constrained to a line.

To arrive at the solution, begin with Eq. (4) and eliminate dependence on the unknown scale by taking the cross-product of both sides with the measurement \mathcal{E}_i . Hence,

$$[\mathscr{C}_i \times] \mathscr{C}_i = [\mathscr{C}_i \times] (p_i - r) \tag{28}$$

Since $\mathbf{r} = r\mathbf{k}$ and $\mathbf{k} = [0, 0, 1]^T$, one finds that

$$\boldsymbol{\ell}_i \times \boldsymbol{p}_i = (\boldsymbol{\ell}_i \times \boldsymbol{k})r \tag{29}$$

Observe that the z-component is zero by construction. Thus, one can remove the 0=0 scalar equation by left-multiplying both sides of the equation by ${\bf S}$

$$S(\mathcal{C}_i \times p_i) = S(\mathcal{C}_i \times k)r \tag{30}$$

where S is given by

$$\mathbf{S} = \begin{bmatrix} \mathbf{I}_{2\times2} & \mathbf{0}_{2\times1} \end{bmatrix} \tag{31}$$

If information from multiple measurements is available, they can be stacked into a set of linear equations to solve for r in the least squares sense:

$$\begin{bmatrix} S(\mathcal{E}_1 \times \mathbf{p}_1) \\ \vdots \\ S(\mathcal{E}_d \times \mathbf{p}_d) \end{bmatrix} = \begin{bmatrix} S(\mathcal{E}_1 \times \mathbf{k}) \\ \vdots \\ S(\mathcal{E}_d \times \mathbf{k}) \end{bmatrix} r \tag{32}$$

Since r is a scalar, it is possible to write the least squares solution directly:

$$r = \frac{\sum_{i=1}^{d} (\boldsymbol{\ell}_{i} \times \boldsymbol{k})^{T} \boldsymbol{B} (\boldsymbol{\ell}_{i} \times \boldsymbol{p}_{i})}{\sum_{i=1}^{d} (\boldsymbol{\ell}_{i} \times \boldsymbol{k})^{T} \boldsymbol{B} (\boldsymbol{\ell}_{i} \times \boldsymbol{k})} = \frac{\sum_{i=1}^{d} (\boldsymbol{\ell}_{i} \times \boldsymbol{k})^{T} (\boldsymbol{\ell}_{i} \times \boldsymbol{p}_{i})}{\sum_{i=1}^{d} (\boldsymbol{\ell}_{i} \times \boldsymbol{k})^{T} (\boldsymbol{\ell}_{i} \times \boldsymbol{k})}$$
(33)

where $\mathbf{B} = \text{diag}(1, 1, 0)$. Using quadruple product identities, this simplifies to

$$r = \frac{\sum_{i=1}^{d} \left((\mathbf{k}^{T} \mathbf{p}_{i}) (\mathbf{\ell}_{i}^{T} \mathbf{\ell}_{l}) - (\mathbf{k}^{T} \mathbf{\ell}_{i}) (\mathbf{\ell}_{i}^{T} \mathbf{p}_{i}) \right)}{\sum_{i=1}^{d} \left((\mathbf{\ell}_{i}^{T} \mathbf{\ell}_{l}) - (\mathbf{k}^{T} \mathbf{\ell}_{i})^{2} \right)}$$
(34)

and then to

$$r = \frac{\sum_{i=1}^{d} \boldsymbol{\ell}_{i}^{T} (\boldsymbol{\ell}_{i} \boldsymbol{k}^{T} - \boldsymbol{k} \boldsymbol{\ell}_{i}^{T}) \boldsymbol{p}_{i}}{\sum_{i=1}^{d} \boldsymbol{\ell}_{i}^{T} \boldsymbol{B} \boldsymbol{\ell}_{i}}$$
(35)

It is possible to solve for r using only a single measurement of an identified point, but observing additional points generally reduces the uncertainty of the result.

VI. Applications

There are a variety of applications of the view invariants introduced in this work, such as localization of trains, aircraft on runways, and interstellar spacecraft. These applications are now briefly considered as a means of illustrating the utility of the ideas presented here. The authors note that this list of applications is not exhaustive and that nearly straight-line trajectories naturally occur in many other situations—such as the final portion of many spacecraft rendezvous trajectories performing a docking (e.g., this technique could also be used to recognize visual features during the final phases of docking with something like the International Space Station).

A. Train on a Straight Track

Improvements in locomotive position estimation allow for more efficient use of rail and shorter transit times. Rail segments are known as cantons. When a train passes over a balise, sensors inform rail traffic management that a train has entered that canton [33]. Trains are also equipped with on-board sensors, such as Doppler radar and wheel sensors, capable of measuring the train's velocity. Classical train localization within a particular canton is accomplished using these velocity measurements and odometry. However, train wheels may slip, adding error to an odometry-based train position estimate. More modern techniques for train localization include Global Navigation Satellite Systems (GNSS) [33–35], eddy current sensors [33], inertial measurement units (IMU) [33,35], and vision-based motion estimation [36]. Of these measurement types, only GNSS measurements are capable of providing the absolute global position of a train. However, GNSS systems are subject to occasional coverage problems, such as when trains travel underground and can no longer detect satellites [33].

The observer position estimation approach outlined in this paper could be used to estimate the distance that a train has traveled along a straight track. This would require that beacon points—visible or infrared (IR) lights, reflectors, or even extant landscape features be placed or located at known 3-D positions along the track and a catalog of their positions be assembled. For example, beacon points can be placed at varying heights along telephone poles (as illustrated in Fig. 4), along the entrances of tunnels or overpasses, or wherever it proves convenient in practice. It is imperative that operators take care to ensure that no two beacons have the same apparent line-ofsight (LOS) plane (i.e., clocking angle). An instrument attached to the train could then collect LOS measurements to one or more beacon points. These beacon points can be uniquely identified and then the train's position can be estimated. Only so many points can be placed along a certain length of straight track before two points will appear to have nearly the same LOS plane. This maximum number is dependent on measurement noise (itself influenced by the smoothness of

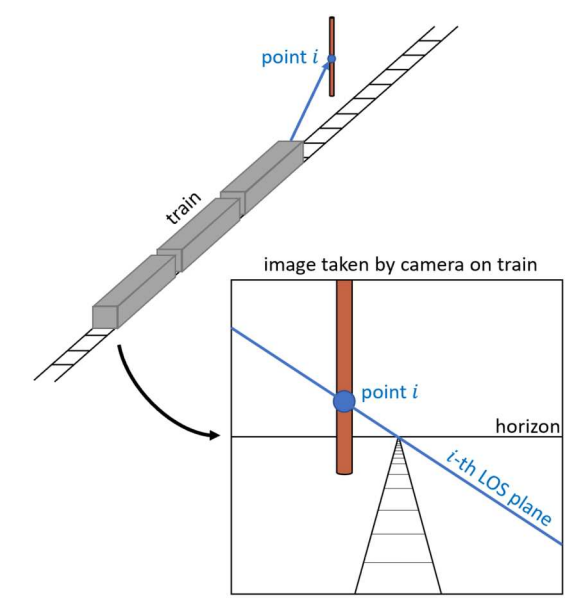


Fig. 4 A train traveling along a straight track can identify natural or artificial beacon points using the methods discussed in this paper.

the train's motion over the track). Artificially installed beacon points will likely only be visible by a fast-moving train for a relatively short time. As such, a train will have to travel a significant distance between beacon point measurements. During periods in which no points are visible, a train can rely on the other position estimation methods mentioned previously.

B. Airplane on a Runway

Commercial aviation could be made safer by improvements to automation during takeoff and landing. This requires that an aircraft be capable of determining its position along a runway, and thus the length of runway remaining. Active research in aircraft navigation includes autonomous navigation for unmanned aerial vehicles (UAVs) or drones, and aircraft tracking on the ground and in the airspace near airports for situational awareness and air traffic control (ATC). The bulk of aircraft ground tracking research is focused on collision avoidance and efficient routing of aircraft to and from runways. Aircraft can be identified and tracked using digital cameras placed around an airport [37–39]. The position and velocity of aircraft can be determined [38], and this information can be fed into a data fusion algorithm such as an extended Kalman filter (EKF) or a multiple hypothesis testing (MHT) algorithm [37,39] to provide ground-side situational awareness at an airport. There are runway detection algorithms to allow aircraft to autonomously identify and track runways in flight from digital images for the purpose of assisted landing [40]. Recent work toward aircraft control during takeoff involves runway centerline tracking [41]. However, autonomous aircraft position estimation on a runway during takeoff and landing remains an open problem.

During takeoff and landing, an aircraft travels along the centerline of a runway with minimal deviation under normal circumstances. An aircraft could use the methods outlined in this paper to estimate its position along a runway. It must be able to take LOS measurements of points placed on or alongside the runway. Most airports are already equipped with lights and navigation beacons for the purpose of assisting pilots. The runway lights flanking either side of a runway could not be used for this purpose, as these are all coplanar with one another and could not be uniquely identified. This method could be employed at major airports that typically service large commercial jets or at smaller airports with no ATC and no other aircraft ground tracking capabilities. Additional lights or beacons can be installed such that they could be detected by an aircraft sensor (see Fig. 5), and the exact positions of these beacons can be made publicly available along with other existing airport information.

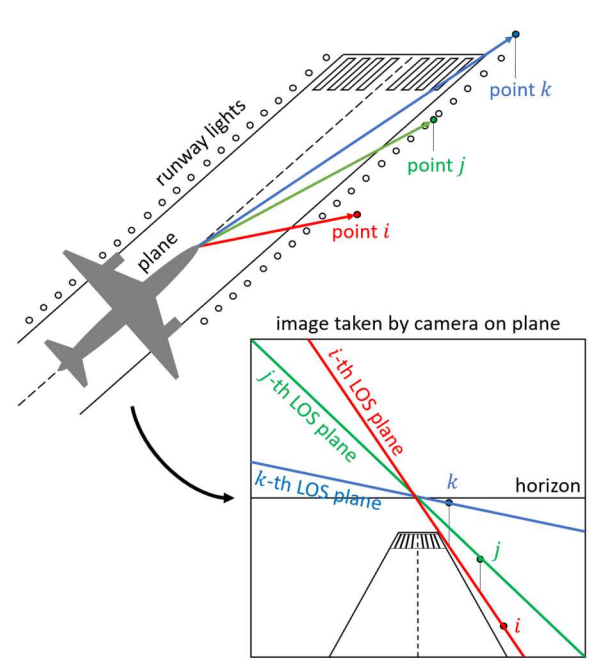


Fig. 5 An aircraft accelerating or decelerating along a runway can identify artificial beacon points on or near the runway using the methods discussed in this paper.

C. Interstellar Spacecraft

Spacecraft navigation is one of the most challenging aspects of interstellar travel due to the immense distances involved [42–44]. A variety of observables have been suggested for interstellar navigation, such as measuring the Doppler shift of stellar spectra [42,44,45], measuring stellar aberration [46], and triangulation with star bearing measurements [42,45]. It is the triangulation-based technique that is of relevance here.

Within the solar system, it is assumed that stars are very far away. Hence, star observations provide little more than observations of reference directions on the celestial sphere, which is usually used for attitude determination (e.g., with star trackers [10,47,48]) or as means of sensor alignment for measurement of foreground objects (e.g., optical navigation [22,49]). Conversely, when an interstellar spacecraft departs the solar system and moves large distances within the Milky Way galaxy, the stars must instead be viewed as 3-D points [11]. This would require construction of a specially designed 3-D star catalog [50] (Fig. 6).

A spacecraft traveling out of the solar system or between stars would be on a very nearly rectilinear trajectory. Thus, observations of stars on an interstellar voyage are exactly the problem of bearing measurements to 3-D points for an observer following rectilinear motion. Ample stars are present in interstellar space, but not all are useful for the technique outlined here. No matter where the spacecraft is located, most stars in the Milky Way galaxy will be too distant for meaningful triangulation Thus, only the closest stars would be useful for spacecraft position estimation (though very distant stars remain quite useful for attitude determination).

If an interstellar spacecraft's trajectory is known, it may be possible to build an invariant index of nearby stars using the method presented here. Given the very large number of stars, special consideration must be given to the possibility of nonunique matches when performing star identification. This challenge may be mitigated by restricting the catalog (and the sensor) to stars brighter than a specified magnitude, which substantially reduces the probability of multiple stars being nearly coplanar. Alternatively, if the number of match hypotheses is small, it may be possible to solve for the spacecraft position for each hypothesis [e.g., using Eq. (35)] and look for solutions that agree with one another.

D. Lost-in-Space Object Identification

The last decade has witnessed a growing interest in autonomous spacecraft navigation using optical sightings of distant space objects,

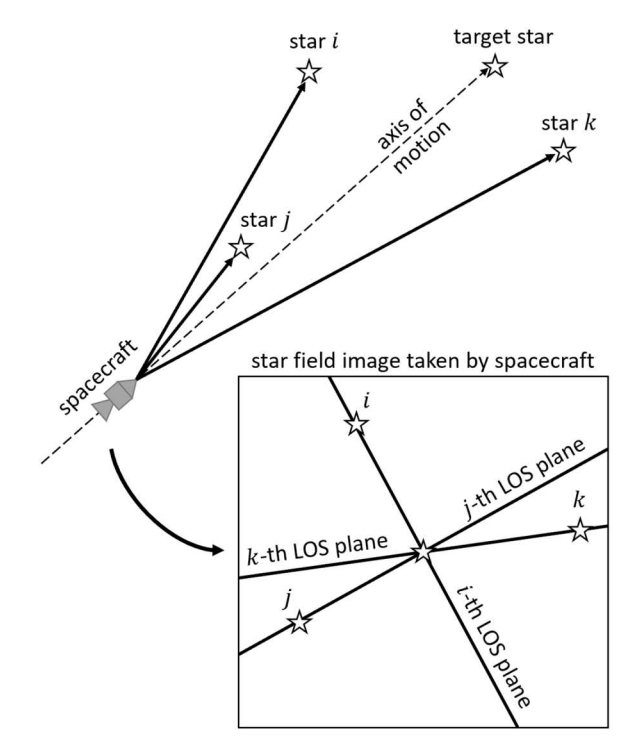


Fig. 6 A spacecraft on a rectilinear interstellar trajectory can identify nearby stars using the methods discussed in this paper.

including both natural celestial bodies (e.g., asteroids, planets, moons) [51–55] and artificial objects (e.g., satellites, human-made surface beacons) [53,56]. The "lost-in-space" problem describes the task of estimating the location of a spacecraft without any a priori information. Given the prior work in navigation with bearings to distant space objects, one may reasonably conjecture that opportunistic sightings of these space objects could be used for lost-in-space navigation (e.g., via triangulation) if they could be matched to a catalog.

Since the objects are assumed distant, they are unresolved and the only available measurement is a bearing direction. In many cases, the locations of the observed objects (either natural or artificial) are quite varied at the scale of interest and one can model this as sightings of 3-D points in general position.

The trajectories for most space missions of interest are not rectilinear. Thus, since the observed 3-D points are assumed to be in general position, it follows that no view invariants exist. The lack of view invariants, in turn, suggests that object identification is not separable from state estimation. This means that it is impossible to match a d-tuple of bearings to a catalog distant 3-D objects without already knowing (or simultaneously solving for) the spacecraft location. The conventional solution would be to randomly guess observation-to-catalog correspondences, compute the camera location, and then validate using residuals and/or additional observations. The combinatorics of this quickly becomes intractable if either the number of observations or number of catalog objects is large. Hence bearings to natural or artificial space objects are unlikely to be a good means of solving the lost-in-space problem. Instead, if the lost-inspace problem must be solved, the analyst may wish to consider other navigation observables to efficiently accomplish this task.

VII. Conclusions

It is well-known that general-case invariants do not exist for a camera viewing an arbitrary set of 3-D points. Invariants may be created by introducing constraints on the general problem, such as constraining all the points to lie on a plane. The novel contribution of this work is the consideration of invariants that arise due to constraints on the camera location. It is shown that the only path that permits invariants is a linear path. Moreover, it is shown that there are d fundamental invariants for a d-tuple of arbitrary points in \mathbb{R}^3 when

measured by an observer constrained to rectilinear motion. Each point in the *d*-tuple has one corresponding invariant, though this can be expressed or computed in a number of ways.

Because there is one invariant property for each point, identification of each point may be achieved with a range query on a 1-D index space. The likelihood of finding a unique match depends on the number of points in the catalog and the sensor noise. Once a point (or set of points) has been identified, it is straightforward to form a linear system to solve for the unknown observer location.

Four applications were explored: train navigation along a straight track, estimation of runway length remaining for an aircraft during takeoff or landing, interstellar spacecraft navigation, and lost-in-space object identification. In each of the first three situations, the techniques outlined this paper could enable autonomous position estimation. In the fourth case, the results of this work highlight the shortcomings of bearing measurements to distance space objects for solving the lost-in-space problem.

Acknowledgment

A portion of H. Derksen's work was supported by NSF grant DMS 2147769.

References

- [1] Koh, S. S., *Invariant Theory*, Springer, Berlin, 1987, pp. 1–7. https://doi.org/10.1007/BFb0078801
- [2] Springer, T. A., *Invariant Theory*, Springer, Berlin, 1977, Vol. 585, pp. 1–14. https://doi.org/10.1007/bfb0095644
- [3] Popov, V. L., and Vinberg, E. B., "Invariant Theory," Algebraic Geometry IV, Springer, Berlin, 1994, pp. 123–278.
- [4] Parshall, K. H., "Toward a History of Nineteenth-Century Invariant Theory," *Ideas and Their Reception*, Elsevier, New York, 1989, pp. 155–206. https://doi.org/10.1016/B978-0-12-599661-7.50013-6
- [5] Derksen, H., and Kemper, G., "Applications of Invariant Theory," Computational Invariant Theory, 2nd ed., Vol. 130, Encyclopaedia of Mathematical Sciences, Springer, Heidelberg, 2015, pp. 265–293. https://doi.org/10.1007/978-3-662-48422-7
- [6] Wolf, J., Burgard, W., and Burkhardt, H., "Robust Vision-Based Localization for Mobile Robots Using an Image Retrieval System Based on Invariant Features," *Proceedings 2002 IEEE International Conference on Robotics and Automation (Cat. No. 02CH37292)*, Vol. 1, Inst. of Electrical and Electronics Engineers, New York, 2002, pp. 359–365. https://doi.org/10.1109/robot.2002.1013387.
- [7] Rothwell, C. A., Object Recognition Through Invariant Indexing, Oxford Univ. Press, Oxford, 1995.
- [8] Brown, M., and Lowe, D. G., "Invariant Features from Interest Point Groups," *British Machine Vision Conference*, Vol. 4, 2002. https://doi.org/10.5244/c.16.23
- [9] Christian, J. A., and Derksen, H., "Invariant Theory as a Tool for Spacecraft Navigation," AAS/AIAA Astrodynamics Specialist Conference, AAS Paper 22-746, Springfield, VA, 2022.
- [10] Christian, J. A., and Crassidis, J. L., "Star Identification and Attitude Determination with Projective Cameras," *IEEE Access*, Vol. 9, 2021, pp. 25,768–25,794. https://doi.org/10.1109/ACCESS.2021.3054836
- [11] McKee, P., Kowalski, J., and Christian, J. A., "Navigation and Star Identification for an Interstellar Mission," *Acta Astronautica*, Vol. 192, 2022, pp. 390–401. https://doi.org/10.1016/j.actaastro.2021.12.007
- [12] Christian, J. A., Derksen, H., and Watkins, R., "Lunar Crater Identification in Digital Images," *Journal of the Astronautical Sciences*, Vol. 68, No. 4, 2021, pp. 1056–1144. https://doi.org/10.1007/s40295-021-00287-8
- [13] Robinson, S. B., and Christian, J. A., "Pattern Design for 3D Point Matching," *Navigation: Journal of the Institute of Navigation*, Vol. 62, No. 3, 2015, pp. 189–203. https://doi.org/10.1002/navi.115
- [14] Christian, J. A., Robinson, S. B., D'Souza, C. N., and Ruiz, J. P., "Cooperative Relative Navigation of Spacecraft Using Flash Light Detection and Ranging Sensors," *Journal of Guidance, Control, and Dynamics*, Vol. 37, No. 2, 2014, pp. 452–465. https://doi.org/10.2514/1.61234

- [15] Burns, J. B., Weiss, R. S., and Riseman, E. M., "The Non-Existence of General-Case View-Invariants," *Geometric Invariance in Computer Vision*, MIT Press, Cambridge, MA, 1992, pp. 120–131.
- [16] Clemens, D. T., and Jacobs, D. W., "Space and Time Bounds on Indexing 3D Models from 2D Images," *IEEE Transactions on Pattern Analysis and Machine Intelligence*, Vol. 13, No. 10, 1991, pp. 1007–1017. https://doi.org/10.1109/34.99235
- [17] Zisserman, A., Forsyth, D., Mundy, J., Rothwell, C., Liu, J., and Pillow, N., "3D Object Recognition Using Invariance," *Artificial Intelligence*, Vol. 78, 1995, pp. 239–288. https://doi.org/10.1016/0004-3702(95)00023-2
- [18] Hilbert, D., "Ueber die Theorie der algebraischen Formen," Mathematische annalen, Vol. 36, No. 4, 1890, pp. 473–534. https://doi.org/10.1007/BF01208503
- [19] Hilbert, D., "Über die vollen Invariantensysteme," Mathematische annalen, Vol. 42, No. 3, 1893, pp. 313–373. https://doi.org/10.1007/BF01444162
- [20] Nagata, M., "On the 14-th Problem of Hilbert," American Journal of Mathematics, Vol. 81, No. 3, 1959, pp. 766–772. https://doi.org/10.2307/2372927
- [21] Hungerford, T. W., Algebra, Springer Science & Business Media, Cham, Switzerland, 1974, Vol. 73, pp. 169–179. https://doi.org/10.1007/978-1-4612-6101-8
- [22] Christian, J. A., "A Tutorial on Horizon-Based Optical Navigation and Attitude Determination with Space Imaging Systems," *IEEE Access*, Vol. 9, 2021, p. 19,819–19,853. https://doi.org/10.1109/ACCESS.2021.3051914
- [23] Christian, J. A., Benhacine, L., Hikes, J., and D'Souza, C., "Geometric Calibration of the Orion Optical Navigation Camera Using Star Field Images," *Journal of the Astronautical Sciences*, Vol. 63, No. 4, 2016, pp. 335–353. https://doi.org/10.1007/s40295-016-0091-3
- [24] Morandi, P., Field and Galois Theory, Vol. 167, Springer-Verlag, New York, 1996, p. 215. https://doi.org/10.1007/978-1-4612-4040-2
- [25] Bentley, J. L., and Friedman, J. H., "Data Structures for Range Searching," *Computing Surveys*, Vol. 11, 1979, pp. 397–409. https://doi.org/10.1145/356789.356797
- [26] Hjaltason, G. R., and Samet, H., "Index-Driven Similarity Search in Metric Spaces (Survey Article)," ACM Transactions on Database Systems, Vol. 28, No. 4, 2003, pp. 517–580. https://doi.org/10.1145/958942.958948
- [27] Mortari, D., "A Fast On-Board Autonomous Attitude Determination System Based on a New Star-ID Technique for a Wide FOV Star Tracker," AAS/AIAA Spaceflight Mechanics Meeting, AAS Paper 96-158, Springfield, VA, 1996.
- [28] Mortari, D., and Neta, B., "k-Vector Range Searching Techniques," AAS/AIAA Spaceflight Mechanics Meeting, AAS Paper 00-128, Spring-field, VA, 2000.
- [29] Christian, J. A., and Arulraj, J., "Review of thek-Vector and Its Relation to Classical Data Structures," *Journal of Guidance, Control, and Dynamics*, Vol. 41, No. 1, 2022. https://doi.org/10.2514/1.G006688
- [30] Hartley, R., and Zisserman, A., Multiple View Geometry, 2nd ed. Cambridge Univ. Press, Cambridge, England, U.K., 2003, pp. 312–323.
- [31] Kaplan, G. H., "Angles-Only Navigation: Position and Velocity Solution from Absolute Triangulation," *Navigation, Journal of the Institute of Navigation*, Vol. 58, No. 3, 2011, pp. 187–201. https://doi.org/10.1002/j.2161-4296.2011.tb02580.x
- [32] Kobylka, K. K., and Christian, J. A., "Methods in Triangulation for Image-Based Terrain Relative Navigation," 31st AAS/AIAA Spaceflight Mechanics Meeting, AAS Paper 21-401, Springfield, VA, 2021.
- [33] Otegui, J., Bahillo, A., Lopetegi, I., and Diez, L. E., "A Survey of Train Positioning Solutions," *IEEE Sensors Journal*, Vol. 17, No. 20, 2017, pp. 6788–6797. https://doi.org/10.1109/JSEN.2017.2747137
- [34] Beugin, J., Legrand, C., Marais, J., Berbineau, M., and El-Koursi, E.-M., "Safety Appraisal of GNSS-Based Localization Systems Used in Train Spacing Control," *IEEE Access*, Vol. 6, 2018, pp. 9898–9916. https://doi.org/10.1109/ACCESS.2018.2807127
- [35] Otegui, J., Bahillo, A., Lopetegi, I., and Díez, L. E., "Evaluation of Experimental GNSS and 10-DOF MEMS IMU Measurements for Train Positioning," *IEEE Transactions on Instrumentation and Measurement*, Vol. 68, No. 1, 2018, pp. 269–279. https://doi.org/10.1109/TIM.2018.2838799
- [36] Tschopp, F., Schneider, T., Palmer, A. W., Nourani-Vatani, N., Cadena, C., Siegwart, R., and Nieto, J., "Experimental Comparison of Visual-Aided Odometry Methods for Rail Vehicles," *IEEE Robotics*

- and Automation Letters, Vol. 4, No. 2, 2019, pp. 1815–1822. https://doi.org/10.1109/LRA.2019.2897169
- [37] Herrero, J. G., Portas, J. B., and Corredera, J. C., "Use of Map Information for Tracking Targets on Airport Surface," *IEEE Transactions on Aerospace and Electronic Systems*, Vol. 39, No. 2, 2003, pp. 675–693.
- https://doi.org/10.1109/TAES.2003.1207274
 [38] Besada, J. A., Garca, J., Portillo, J., Molina, J. M., Varona, A., and Gonzalez, G., "Airport Surface Surveillance Based on Video Images," *IEEE Transactions on Aerospace and Electronic Systems*, Vol. 41, No. 3, 2005, pp. 1075–1082. https://doi.org/10.1109/TAES.2005.1541452
- [39] Dimitropoulos, K., Grammalidis, N., Simitopoulos, D., Pavlidou, N., and Strintzis, M., "Aircraft Detection and Tracking Using Intelligent Cameras," *IEEE International Conference on Image Processing 2005*, Vol. 2, Inst. of Electrical and Electronics Engineers, New York, 2005, pp. 592–594. https://doi.org/10.1109/ICIP.2005.1530125
- [40] Gong, X., Abbott, L., and Fleming, G., "A Survey of Techniques for Detection and Tracking of Airport Runways," 44th AIAA Aerospace Sciences Meeting and Exhibit, AIAA Paper 2006-1436, 2006. https://doi.org/10.2514/6.2006-1436
- [41] Sadien, E., Roos, C., Birouche, A., Carton, M., Grimault, C., Romana, L. E., and Basset, M., "A Simple and Efficient Control Allocation Scheme for On-Ground Aircraft Runway Centerline Tracking," *Control Engineering Practice*, Vol. 95, June 2020, Paper 104228. https://doi.org/10.1016/j.conengprac.2019.104228
- [42] Moskowitz, S., and Devereux, W., "Trans-Stellar Space Navigation," AIAA Journal, Vol. 6, No. 6, 1968, pp. 1021–1029. https://doi.org/10.2514/3.4668
- [43] Strong, J., "Trans-Stellar Navigation." Spaceflight, Vol. 13, No. 4, 1971, pp. 252–255.
- [44] Wertz, J., "Interstellar Navigation," Spaceflight, Vol. 14, No. 6, 1972, pp. 206–216.
- [45] Yucalan, D., and Peck, M., "Autonomous Navigation of Relativistic Spacecraft in Interstellar Space," *Journal of Guidance, Control, and Dynamics*, Vol. 44, No. 6, 2021, pp. 1–10. https://doi.org/10.2514/1.G005340
- [46] Christian, J. A., "StarNAV: Autonomous Optical Navigation of a Spacecraft by the Relativistic Perturbation of Starlight," *Sensors*, Vol. 19, Oct. 2019, p. 4064. https://doi.org/10.3390/s19194064

- [47] Liebe, C. C., "Star Trackers for Attitude Determination," *IEEE Aerospace and Electronic Systems Magazine*, Vol. 10, No. 6, 1995, pp. 10–16. https://doi.org/10.1109/62.387971
- [48] Liebe, C. C., "Accuracy Performance of Star Trackers—A Tutorial," IEEE Transactions on Aerospace and Electronic Systems, Vol. 38, No. 2, 2002, pp. 587–599. https://doi.org/10.1109/TAES.2002.1008988
- [49] Owen, W., "Methods of Optical Navigation," AAS/AIAA Space Flight Mechanics Meeting, AAS Paper 11-215, Springfield, VA, 2011.
- [50] Wu, L., "Guide Star Catalog Generation of Star Sensors for Interstellar Navigation," *Journal of Astronomical Telescopes, Instruments, and Systems*, Vol. 6, No. 4, 2020, Paper 044006. https://doi.org/10.1117/1.JATIS.6.4.044006
- [51] Karimi, R. R., and Mortari, D., "Interplanetary Autonomous Navigation Using Visible Planets," *Journal of Guidance, Control, and Dynamics*, Vol. 38, No. 6, 2015, pp. 1151–1156. https://doi.org/10.2514/1.G000575
- [52] Broschart, S. B., Bradley, N., and Bhsakaran, S., "Kinematic Approximation of Position Accuracy Achieved Using Optical Observations of Distant Asteroids," *Journal of Spacecraft and Rockets*, Vol. 56, No. 5, 2019, pp. 1383–1392. https://doi.org/10.2514/1.A34354
- [53] Bradley, N., Olikara, Z., Bhsakaran, S., and Young, B., "Cislunar Navigation Accuracy Using Optical Observations of Natural and Artificial Targets," *Journal of Spacecraft and Rockets*, Vol. 57, No. 4, 2020, pp. 777–792. https://doi.org/10.2514/1.A34694
- [54] Hinga, M. B., "Cis-Lunar Autonomous Navigation via Implementation of Optical Asteroid Angle-Only Measurements," 21st Advanced Maui Optical and Space Surveillance Technologies (AMOS) Conference, 2020.
- [55] Franzese, V., and Topputo, F., "Optimal Beacons Selection for Deep-Space Optical Navigation," *Journal of the Astronautical Sciences*, Vol. 67, No. 4, 2020, pp. 1775–1792. https://doi.org/10.1007/s40295-020-00242-z
- [56] Driedger, M., and Ferguson, P., "Feasibility Study of an Orbital Navigation Filter Using Resident Space Object Observations," *Journal of Guidance, Control, and Dynamics*, Vol. 44, No. 3, 2021, pp. 622–628. https://doi.org/10.2514/1.G005210